J Solid State Electrochem (2007) 11:1531–1539
DOI 10.1007/s10008-007-0348-7

ORIGINAL PAPER

Bulk CO oxidation on platinum electrodes vicinal to the Pt(111) surface

Camilo A. Angelucci · Enrique Herrero · Juan M. Feliu

Received: 14 February 2007 / Revised: 9 April 2007 / Accepted: 26 April 2007 / Published online: 31 May 2007

Abstract Bulk CO oxidation has been studied on platinum stepped surfaces belonging to the series Pt(S)[*n*(111)×(111)], using a hanging meniscus rotating disk electrode (HMRDE) configuration. The general shape of the voltammograms is not significantly affected by the presence of the steps. However, the curves shift towards negative values as the step density increases. Thus, in the positive-going scan, a linear relationship is observed for the dependence of the potential for the ignition peak vs the step density for surfaces with terraces wider than five atoms, shorter terraces deviate from this behavior. In the negative-going scan, a similar situation is observed for the potential where the current drops to zero. In this case, Pt(111) electrode also deviates from the expected behavior because of the formation of the ordered bisulfate adlayer on the electrode. The anion readsorption process is also observed by recording the HRMDE voltammograms at a high scan rate. All these results have been analyzed in light of a common mechanism, discussing the possible role of the steps in the stability and reactivity of the CO adlayer.

Introduction

The oxidation of CO on well-defined platinum electrodes is one of the most studied reactions in surface electrochemistry. CO is not only a widely used surface probe but also the most frequent poison in electrocatalysis, and therefore, its elimination reaction has both applied and fundamental interest. A great number of papers deal with the oxidation of adsorbed CO, i.e., in absence of CO in the solution phase, which takes place in a sharp, ignition peak at high potential values. As the reaction product, CO_2, is not adsorbed on the surface, the electrode readily reaches the state of charge of the blank electrode after the stripping of the CO monolayer. This double layer correction has to be taken into account when coulometric studies are attempted [1].

On Pt(111) electrodes, the maximum stable coverage for adsorbed CO in the absence of CO in a solution is about 0.68, which agrees with the (√19×√19)- 13CO structure [2–8], and involves an oxidation charge of 320 μC cm^{-2}. This charge is associated to two different charge transfer processes, namely, the CO oxidation:

$$Pt - CO + H_2O \rightarrow Pt + CO_2 + 2H^+ + 2e \quad (1)$$

and the anion adsorption at the free sites:

$$Pt + A^- \rightarrow Pt - A + e \quad (2)$$

as anions are readily adsorbed on the electrode surface at the potential where the CO oxidation takes place. Therefore, anions play a significant role in the oxidation process. Several kinetic studies on Pt(111) electrodes indicate that the

In memoriam of Francisco C. Nart, an excellent scientist, colleague, and friend.

C. A. Angelucci
Instituto de Química de São Carlos, Universidade de São Paulo,
P.O. Box 780, 13560-970 São Carlos, SP, Brazil

E. Herrero · J. M. Feliu (✉)
Instituto de Electroquímica, Universidad de Alicante,
Apdo. 99,
E-03080 Alicante, Spain
e-mail: juan.feliu@ua.es

oxidation process follows a Langmuir–Hinshelwood (L-H) mechanism involving the following steps:

$$Pt + H_2O \rightleftharpoons Pt - OH + H^+ + e \quad (3)$$

$$Pt - OH + Pt - CO \rightarrow CO_2 + H^+ + e + 2Pt \quad (4)$$

The kinetics of CO oxidation on Pt single crystal electrodes has been extensively studied in recent years [9–18]. These studies have revealed that the CO oxidation on Pt(111) and vicinal electrodes takes place according to the mean field L-H type mechanism [14–18]. Because the oxidation process takes place at very localized sites, where OH_{ads} and CO_{ads} species can interact, the mean field L-H type mechanism is fulfilled only if CO diffusion on the surface is fast [19]. It has also been observed that defects play a critical role in the oxidation process. An extrapolation of the rate constants for the CO_{ads} oxidation obtained with the Pt(111) vicinal electrodes to the "ideal" (defect-free) Pt(111) electrode indicates that the oxidation on real Pt(111) electrodes takes place almost exclusively at the defect sites [16]. It has been proposed that the OH adsorption takes place on the step site, reacting with a CO molecule adsorbed on a terrace site close to the step [20].

This characteristic electrochemical behavior can also be observed when the experiments are made in CO-containing solutions [21–23] usually under a rotating disk arrangement. Using the Pt(111) electrode as an example, it can be seen that the surface is initially blocked until the ignition peak appears at a potential of about 100 mV higher than in absence of CO in the solution, because in the latter case, the adlayer structure is (2×2)- 3CO, and the coverage is higher (0.75) [2, 7]. However, the current does not drop to zero as bulk CO oxidation takes place after the ignition peak. In the negative-going sweep, CO oxidation continues, even at potentials lower that those of the ignition peak, suggesting that the compact adsorbed layer is not yet formed, leaving places for OH adsorption and allowing the upcoming CO to react. The currents measured in this region are affected by the presence of the anions [2], and depending on the experimental condition, oscillatory behavior has been described [23]. In a recent paper [24], anions were shown to play a role in the kinetics of this process.

Although the bulk CO oxidation should be governed by the same parameters than the adsorbed CO oxidation, there are some differences that can modify the expected behavior. First of all, the adsorbed CO layer has a different structure, leading to a higher coverage. On stepped surfaces having (111) terraces, the compact structure survives until the onset of CO oxidation according to infrared (IR) data [25]. The other important difference is that the anions are interfering with the oxidation in the whole potential range but especially in the region after the ignition peak. To study the effect of the long-range order and the presence of steps in the oxidation of bulk CO, we have studied this reaction on platinum stepped electrodes vicinal to the (111) surface.

Experimental

Platinum single crystal electrodes vicinal to the (111) pole were oriented, cut, and polished from small single crystal platinum beads (2.5 mm diameter) following the procedure described by Clavilier et al. [26]. The surfaces used were Pt (111) itself and those belonging to the series of Pt(S)[*n* (111)×(111)], having Miller indices Pt(*n*,*n*,*n*-2) simplified in the usual way. These surfaces can be also regarded as Pt (S)[(*n*−*1*)(111)×(110)] because the junction of a (111) step site with the (111) terrace forms a (110) site. As usual, *n* represents the number of terrace atoms. The electrodes were cleaned by flame annealing and cooled down in H_2/Ar and protected with water in equilibrium with this gas mixture to prevent contamination before immersion in the electrochemical cell, as described elsewhere [27]. It has been shown that this procedure leads to surface topographies reasonably close to the nominal ones [28, 29]. The theoretical step density of these electrodes is defined by:

$$N_{(111)\times(111)} = \frac{2}{\sqrt{3}d\left(n - \frac{2}{3}\right)} \quad (5)$$

where d is the platinum atomic diameter and is equal to 0.278 nm. The voltammetric profile in 0.1 M H_2SO_4 is shown in Fig. 1.

CO oxidation experiments have been performed on well-defined platinum surfaces under the hanging meniscus rotating disk electrode (HMRDE) configuration and most experimental details have been described previously [30]. To avoid any particular effect of the immersion potential on the CO oxidation response, which has been indeed observed, only the stationary behavior is discussed. Special care has been taken to maintain the electrode surface order during the whole experiment. The preservation of the surface order was checked by comparison of the initial and final fingerprint voltammograms in solutions free of CO. The selection of the upper potential limit of the sweep is particularly crucial to achieve this point.

Experiments were carried out at room temperature, 22 °C, in classical two-compartment electrochemical cells, including a platinum counter-electrode and a reversible hydrogen

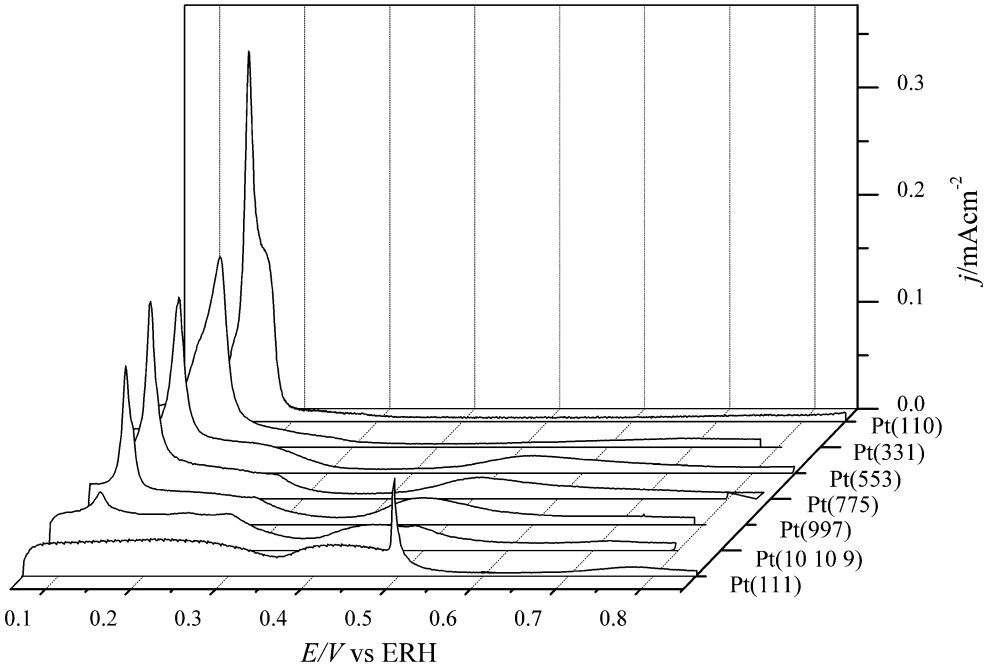

Fig. 1 Positive-going voltammetric profiles of the electrodes used in this work in 0.1 M H_2SO_4. Scan rate, 50 mV s^{-1}

(N50) electrode (RHE) as reference. Solutions were prepared from concentrated sulfuric acid (doubly distilled, Aldrich) and ultrapure water from Elga. When necessary, solutions were deoxygenated using Argon (Air Liquide, N50). CO-saturated solutions were prepared using CO (Air Liquide, N48). The cleanliness of the solutions was tested by the stability of the characteristic voltammetric features of well-defined Pt(111) electrodes in deoxygenated solutions.

Results and discussion

The voltammetric profile for bulk CO oxidation on the stepped surfaces is shown in Fig. 2. The general shape of the voltammograms is very similar in all cases. As can be seen, the oxidation of CO does not take place under stationary conditions in the potential range below 0.85 V in the positive going sweep until the ignition process takes

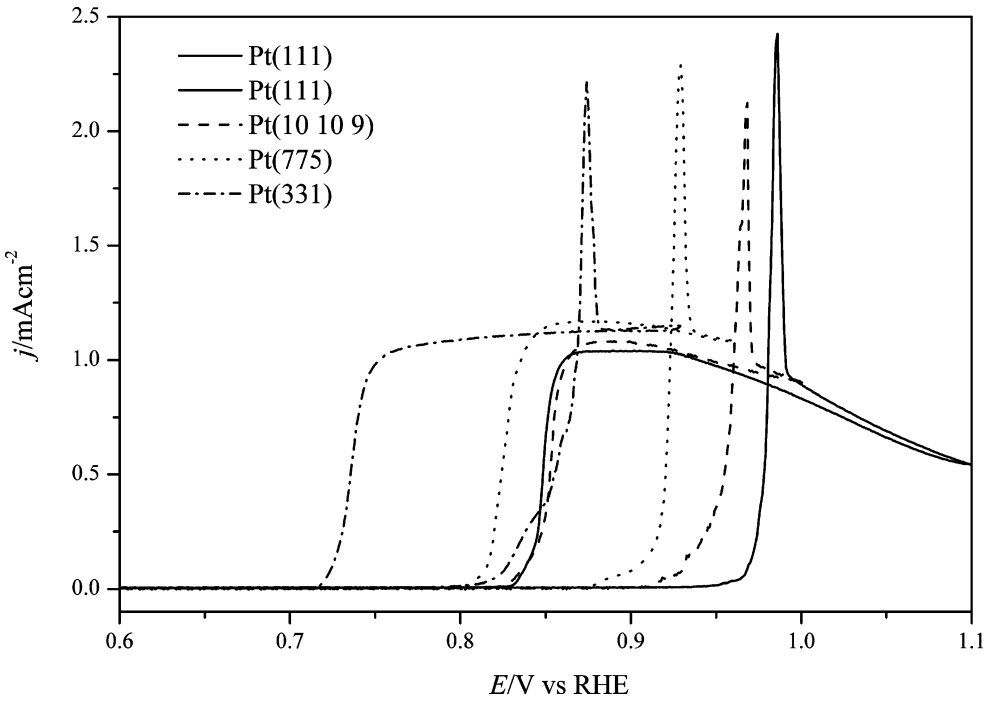

Fig. 2 Saturated CO-bulk oxidation voltammograms corresponding to the Pt(111) and some stepped surface electrodes in 0.1 M H_2SO_4 at 20 mV s^{-1} and 600 rpm

place, and the current jumps sharply. This reaction involves adsorbed CO and also concomitant bulk CO oxidation on the fresh platinum free sites. In this ignition peak, anion adsorption can readily take place because the potential is quite high with respect to the pztc values measured in this electrolyte [31]. Then, the surface becomes essentially free of adsorbed CO, as proven by the diffusion-controlled constant plateau recorded in the positive and negative going sweeps for the stepped surfaces. A small diminution of the current is observed for the Pt(111) electrode likely because of the adsorption of a particularly stable sulfate adlayer [32] that would affect the formation of adsorbed OH. With the exception of Pt(111), the upper potential limit has to be reversed at 1.00 V to avoid oxygen adsorption and subsequent disordering of the surface.

The flat current plateau in the negative-going sweep also indicates that the bulk oxidation process still remains controlled by mass transport. As the current density values in the plateau region agree with those calculated for a diffusion-controlled process, we can accept that the oxidation of CO is a fast process under these conditions. Thus, the CO coverage should remain negligible in the whole plateau region ($\theta_{CO} \rightarrow 0$). At potentials lower than 0.78 V, the surface becomes blocked again by CO: The diminution of the CO oxidation rate leads to the buildup of a CO layer as the oxidation rate is smaller than the adsorption rate. This is because OH adsorption is a potential dependent process also influenced by anion adsorption, which in turn is also a potential dependent process. The most significant differences in the voltammograms for bulk CO oxidation on these surfaces are related to the change in potential of the ignition peak in the positive-going scan and the current drop in the negative going one that can be monitored by its half-wave potential. Both processes move towards lower potentials as the step density increases, i.e., the Pt(331) electrode has the lowest potential values for the ignition peak and the potential drop (which are, indeed, very close to that of Pt(110) [22]), whereas the highest potentials are observed for the Pt(111) electrode.

The shape of the voltammograms and the differences observed for the stepped surfaces are consequences of the general mechanism of the reaction. Under a simplified approach, three main processes can be distinguished for the overall reaction. The first one is the diffusion of the CO from the bulk of the solution to the electrode surface:

$$CO_{bulk} \rightarrow CO_{surf} \tag{6}$$

and the diffusion rate can be written as:

$$v_{dif} = D_{CO} \frac{c_{CO}^{bulk} - c_{CO}^{surf}}{\delta} \tag{7}$$

where δ is the mean thickness of the diffusion layer and, according to previous works with the same electrode configuration [30], is very close to the value obtained for the rotating disk electrode given by Levich's equation.

The second process in the reaction is the CO adsorption on the electrode surface according to:

$$CO_{surf} \rightarrow CO_{ads} \tag{8}$$

In this case, the adsorption rate constant for CO is high, and we can consider that almost any CO molecule in the vicinity of the electrode surface will be immediately adsorbed, provided that there are some free sites for adsorption on the electrode surface. The reaction rate is then:

$$v_{ads} = k_{ads} c_{CO}^{surf} (1 - \theta_{CO}) \tag{9}$$

where θ_{CO} is the fraction of Pt sites covered by CO_{ads}. The competition of the desorption step to the whole adsorption rate can be considerably negligible under the present experimental conditions. It should be mentioned that the maximum CO coverage for Pt(111), Θ_{CO}, defined as the ratio of the number of adsorbed CO molecules to the number of Pt surface sites, is 0.75. This CO coverage corresponds to a situation where θ_{CO}=1, as all the Pt sites are blocked by CO.

The final process is the oxidation of the adsorbed CO according to:

$$CO_{ads} + H_2O \rightarrow CO_2 + 2H^+ + 2e \tag{10}$$

This process has to be decomposed into several elementary steps, as depicted in reactions 3 and 4, which are in competition with reaction 2 [14–18]. These steps include water dissociation to yield adsorbed OH and the reaction of adsorbed CO with adsorbed OH. However, to simplify, it is more convenient to maintain Eq. 10 as a whole unit. The reaction rate for this process can be finally described by the L-H mean field mechanism:

$$v_{reac} = k_{reac} \Theta_{CO} (1 - \theta_{CO}) \tag{11}$$

where k_{reac} is the rate constant, which, obviously, depends on the applied potential. For Pt(111) and the stepped surfaces, the measured Tafel slope is ca. 75 mV [16]. The implicit assumption in this equation is that the OH_{ads} coverage is proportional to the fraction of free sites not

covered by CO in the whole relevant potential region. In this respect, OH adsorption depends on anion adsorption and mainly on the presence of surface steps. The simplest case is that in which OH adsorption on step sites takes place at the same rate independently of the terrace length. This should be true for electrodes with low step density, in which the distance between the steps is large. Deviations may be expected when the terraces become narrower, because the electrical interaction between the step dipoles (Smoluchowski effect) would be nonnegligible [33]. It should be mentioned that the oxidation of CO would be completely inhibited for a perfect CO layer, i.e., if θ_{CO}=1. Therefore, the initial stages of the oxidation process are always linked to the presence of defects. Incidentally, it has been demonstrated that the increasing number of defects on Pt(111) electrode surfaces results in a shift of the peak for adsorbed CO oxidation (in the absence of CO in solution) toward lower potentials [16].

The voltammetric profile is then a consequence of a delicate balance between the three relevant step rates. At low potentials, the surface is immediately covered by CO as the reaction rate is very low, and a compact CO layer is formed in all cases. For the stepped surfaces vicinal to the (111) pole with n>5, IR spectra have the same absorption characteristics of the (2×2)- 3CO structure found for the Pt (111) electrode in the presence of CO in solution [20], for which the CO coverage is 0.75 [31]. Therefore, for the stepped surfaces with large terraces, the surface structure of the adsorbed CO is expected to be very similar to that found on the Pt(111) electrode. As the potential is made more positive, the k_{reac} will increase, and some adsorbed CO molecules will be oxidized in the zones where defects are found. In absence of CO in the solution, this will trigger the apparition of a sharp voltammetric peak for the oxidation of the CO layer. However, in the presence of CO in solution, the free sites created by the oxidation of CO_{ads} will be readily covered again by the adsorption of CO molecules also in competition with anions until the reaction rate would be higher than the adsorption rate of CO on the free sites. At this moment, the ignition peak will appear (Fig. 2), i.e., with a higher peak potential as compared to that in the absence of CO in the solution side. Therefore, the potential for the ignition peak is controlled by three main factors, k_{reac}, k_{ads}, and the initial number of defects in the CO layer. Assuming that the differences in k_{ads} for the different sites present on the platinum electrodes are small, the position of the ignition peak would be mainly controlled by the number of defects and k_{reac}.

Figure 3 shows the evolution of the ignition peak potential vs the step density. As expected, there is a linear diminution of the potential with the step density, which deviates slightly for narrow terraces. For the Pt(553) electrode, the observed behavior starts to deviate from the

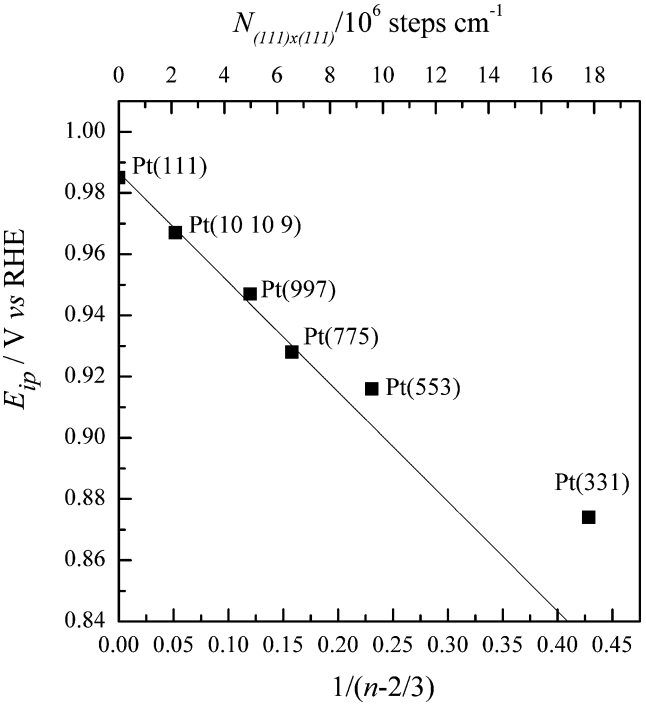

Fig. 3 Potential of the ignition peak vs the step density for the different electrodes

extrapolated behavior. The deviation is greater for Pt(331) and has been observed in other cases [33]. This effect must be consequence of the presence of short terraces. For long terraces, the modification in the surface energy caused by the presence of the step only affects a small fraction of the terrace. For shorter terraces, this modification extends over the whole terrace, and there can even be a coupling effect between two neighboring steps. Therefore, it is expected that their behavior deviate from that observed for surfaces with long terraces. This kind of deviations has been observed when measuring the work function of the electrodes [31] or for the catalytic behavior of these surfaces for formic acid dissociation [34]. Incidentally, this can be seen in the step-related peak at 0.12 V (Fig. 1), which becomes wider and exhibits different contributions for electrodes having short terraces.

In this case, it is very difficult to indicate whether the variation of k_{ads} is the dominant parameter in the observed behavior. It is known that the measured k_{reac} depends linearly on the step density for the stepped surfaces vicinal to the (111) electrode [16], which is in agreement with the observed behavior. However, the presence of defects in the adlayer should also increase as a function of the step density because of the disruption of the long order at the step. In fact, both factors can be regarded as two sides of the same coin: the presence of steps. The step is the place where the oxidation of CO preferentially takes place and

also breaks the long range order of the CO adlayer. In addition, the presence of steps also modify the anion adsorption, but this effect can be considered as a minor perturbation at this stage. A special situation will be described below, for the case of Pt(111), that is largely the most ordered surface used in this study.

After the ignition peak, the oxidation rate is high and every molecule that reaches the surface will be immediately oxidized. Therefore, the limiting current density should be measured in this region. When compared to the currents measured in perchloric acid [22] in this potential region, currents in sulfuric acid media are slightly smaller and diminish as the potential increases, especially for Pt(111). This fact indicates that the anion adsorption should play a competitive role in the measured reaction rate. The observed effect is similar to that in chloride media but to a much lesser extent because the sulfate layer is quite open [22]. The diminution can be then associated to an increasing difficulty for the dissociation of water to yield adsorbed OH. The main fact is that, irrespectively of minor modifications because of the role of the anion, θ_{CO} can be considered to remain negligibly small in this potential region.

In the negative scan, the currents rise again, or remain constant, for the different stepped surface electrodes. Significant currents are measured at potentials negative to the ignition peak thus showing that the compact CO adlayer cannot be formed. At a given potential, which depends on the electrode surface and indeed of anion adsorption, OH_{ads} formation decreases, and the current sharply decreases. In this moment, the v_{reac} is lower than the diffusion rate, and the incoming CO molecules cannot be oxidized and remain adsorbed on the surface, giving rise to a self-poisoning effect. According to the proposed mechanism, the potential for the inhibition of the CO oxidation depends on the balance between v_{reac} and v_{dif}, always assuming that the CO adsorption constant (k_{ads}) is the same for all the surfaces. In the comparison between the stepped surfaces, the diffusion rate is the same for all the electrodes (the rotation rate is constant), and therefore, the differences have to be due to the differences in v_{reac} through the rate of formation of the partner OH_{ads}. Figure 4 shows the half-wave potential (defined as the potential at which the current density in the negative scan is half of the stationary current density measured in the same scan) vs the step density. As can be seen, the half-wave potential diminishes as the step density increases. A linear behavior is observed for all the stepped surfaces with long terraces. As before, surfaces with short terraces deviate from the general behavior. It is noteworthy that Pt(331) strongly deviates from the general trend. The behavior of this surface, the turning point of the crystallographic zone, is quite similar to that of Pt(110) [23]. The higher concentration of (110) sites may be responsible of this particular behavior.

Unexpectedly, the Pt(111) electrode also deviates from the linear plot. As can be seen, the potential is very similar to that measured for the Pt(10,10,9) electrode. It is known

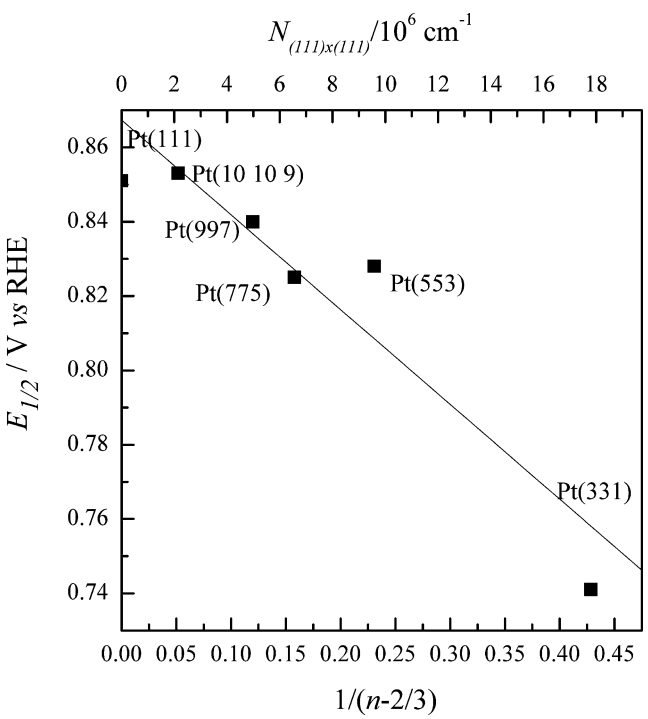

Fig. 4 Half-wave potentials for the current drop in the negative-going scan vs the step density for the different electrodes

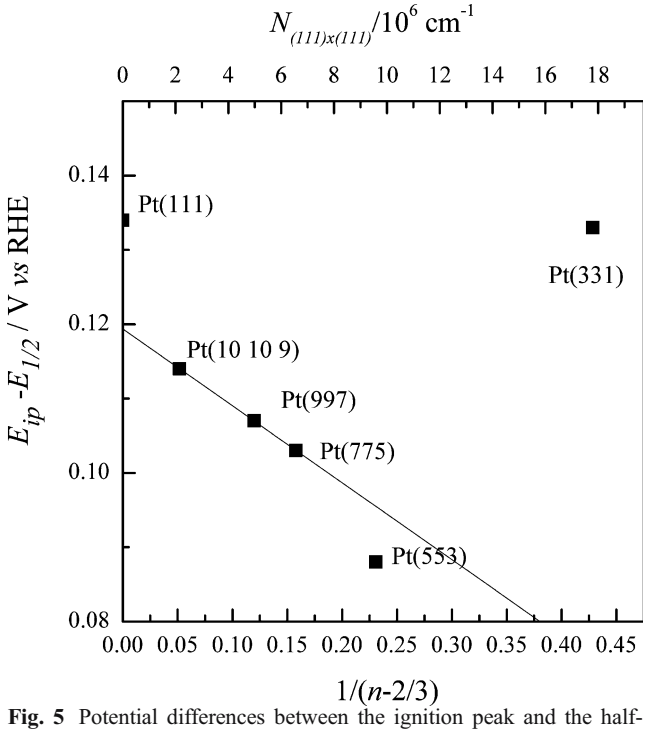

Fig. 5 Potential differences between the ignition peak and the half-wave potential for the current drop in the negative-going scan vs the step density for the different electrodes

that reaction rate for CO oxidation is proportional to the step density or the number of non-(111) terrace sites present on the surface. The similar potential for both electrodes would indicate that the number of defects in the Pt(111) electrode used in this work is quite high. However, the voltammetric profile of the Pt(111) electrode clearly shows that the number of defects is lower than 1% (see Fig. 1). For this electrode, the presence of defects is associated to the apparition of the peak at 0.12 V potential, which coincides with that corresponding to the step sites in this series of stepped surfaces or at 0.27 V that would be corresponding to steps with (100) symmetry. These peaks are almost undetectable for this particular Pt(111) electrode and, definitively, are much smaller than the contributions observed at these potentials for the Pt(10,10,9) electrode. Thus, the number of defects for the Pt(111) is then much lower than that of the number of step sites on the Pt (10,10,9) surface, and the similar v_{reac} cannot be justified by the presence of a similar number of non-(111) terrace sites. The important difference between both surfaces that can justify the differences is the formation of a well-ordered sulfate adlayer on the Pt(111) electrode. This is revealed by the presence of the sharp spike at 0.48 V in the voltammograms in sulfuric acid solutions, which is less noticeable in the rest of the voltammograms. This sharp spike is related to the disorder/order transition of the sulphate adlayer [32]. The formation of a particularly long-range ordered sulfate adlayer implies additional stabilization energy. For that reason, CO adsorption is more difficult, and the decay in the current takes place at potentials 16 mV more negative than the expected values. A similar effect is observed for oxygen reduction in the same series of stepped surfaces [30]. In this case, the formation of the ordered adlayer also shifts the half-wave potential for oxygen reduction to negative values in comparison to what would be expected for the extrapolated behavior obtained from stepped surfaces having wide terraces.

The role of the defect density in the oxidation of the CO adlayer can be examined by plotting the potential difference between the ignition peak and the half-wave potential for

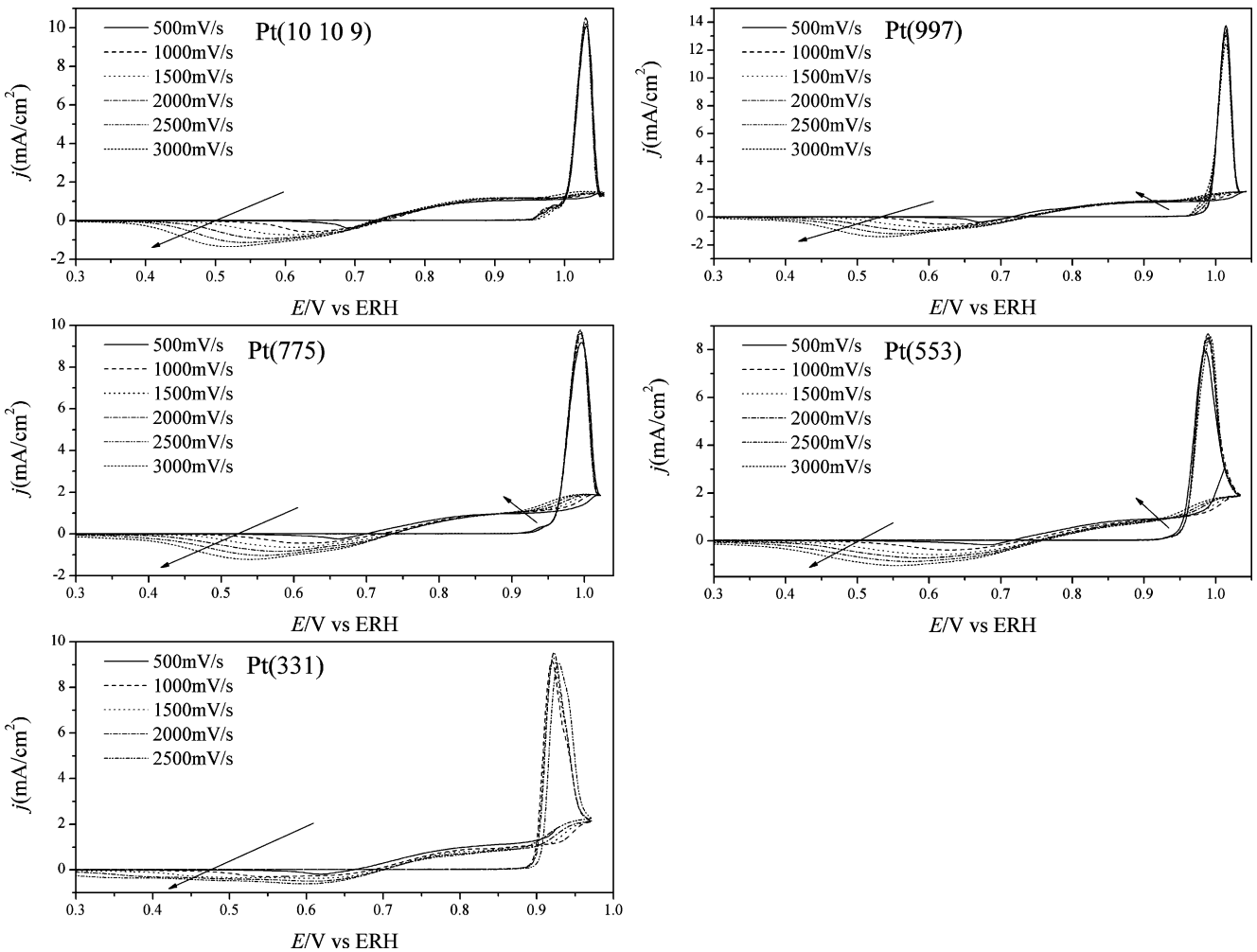

Fig. 6 Cyclic voltammetry for the stepped surfaces in a CO-saturated 0.1 M H_2SO_4 solution at 600 rpm, 500 mV/s in the positive-going sweep, and different scan rates in the negative-going sweep. The *arrows* indicate the effect of the increasing scan rate

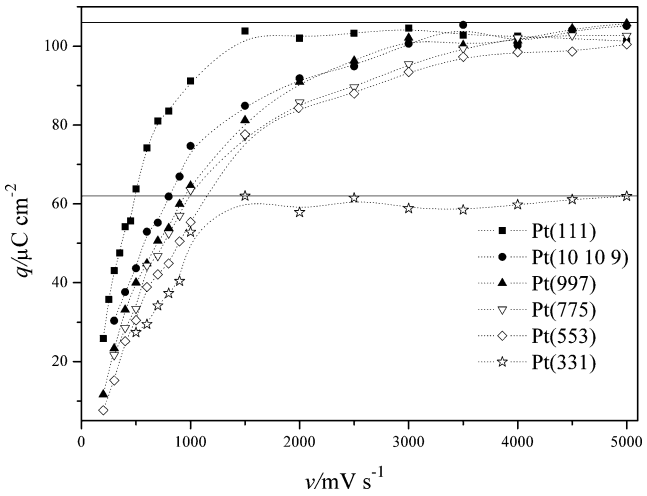

Fig. 7 Plot of the charge density calculated from integration of peak in negative scan vs the scan rate for the different electrode. The *horizontal lines* correspond to the CO displacement experiments in the same electrolyte including free charge contributions for Pt(111) and Pt (311) electrodes

the current decay vs the step density (Fig. 5). As the first one depends on k_{reac} and the number of defects and the latter is proportional only to k_{reac}, the difference between both will be mainly the function of the number of defects. As can be seen, a linear behavior is observed for the stepped surfaces with longer terraces, and again, Pt(111) electrode deviates from the expected value, owing to the low value for the half-wave potential.

From the above results, anions are expected to be adsorbed on the electrode surfaces in the potential range between the end of the ignition step in the positive-going sweep and the drop of the bulk CO oxidation in the negative-going one. Thus, anions have to be displaced from the surface as CO blocks it in a similar way as they are desorbed in the CO displacement experiment, which is usually carried out at much lower potentials [33]. To get insight into the anion displacement process, a series of experiments were performed at a constant rotation rate of 600 rpm but at an increasing sweep rate, in the negative-going sweep, for the series of stepped surfaces (Fig. 6). It is clear that, at increasing sweep rates, the ignition process would take place at higher potentials, and for this reason, the positive-going sweep was kept constant. The diffusion controlled rate of bulk CO oxidation remains nearly constant in the negative-going sweep, which is diffusion process controlled by the electrode rotation. If sulfate anions are adsorbed in the mass transport controlled region ($\theta_{CO} \rightarrow 0$) and maintaining constant the CO flux by the rotation rate, the CO will reach the anion covered surface in the potential region in which it could not be oxidized (there is no more OH_{ads}). Then CO will adsorb and thus displace the sulfate anions adsorbed at the interface. This will happen at high sweep rates in the negative-going direction. At progressively high scan rates, net reduction currents that increase with the sweep rate are observed. These negative currents have also been observed in other papers dealing with bulk CO oxidation on platinum [6, 21]. Previous studies with the Pt(111) electrodes indicate that the net reduction currents involve a charge density that fits with the reductive displacement of the adsorbed anions by CO [23] according to:

$$Pt - A + CO + e \rightarrow Pt - CO + A^- \quad (12)$$

Thus, the presence of CO in the solution forces the anion displacement at these high potentials. The charge densities integrated in the negative-going sweep, taking into account the effect of the sweep rate in the time scale, are given by:

$$q = \int j dt = \int \frac{j}{v} dE \quad (13)$$

These charges increase with the sweep rate until a constant value is reached (Fig. 7). All the results fit remarkably well with the hypothesis that anion displacement by CO is at the origin of the reduction charge density displaced in the negative-going sweep.

Conclusion

As a conclusion, steps have a great influence in the oxidation processes observed in CO-containing solutions. Preliminary kinetics studies suggest that either the ignition of adsorbed CO in the positive-going sweep and the current drop of bulk CO oxidation in the negative-going one linearly depend on the step density. The role of the anions can be pointed out at increasing negative-going sweep rates because the anion displacement by CO leads to reduction currents. The measured charge densities reach constant values at high sweep rates, indicating a surface-controlled process similar to that measured in absence of CO in the solution.

Acknowledgments This work is financially supported by MEC (project nos. PHB2005-0054-PC and CTQ2006-04071/BQU; Spain) and FAPESP, Capes, and CNPq (Brazil).

References

1. Gomez R, Feliu JM, Aldaz A, Weaver MJ (1998) Surf Sci 410:48
2. Villegas I, Weaver MJ (1994) J Chem Phys 101:1648
3. Oda I, Inukai J, Ito M (1993) Chem Phys Lett 203:99
4. Villegas I, Weaver MJ (1994) J Electroanal Chem 373:245
5. Lucas CA, Markovic NM, Ross PN (1999) Surf Sci 425:L381
6. Markovic NM, Grgur BN, Lucas CA, Ross PN (1999) J Phys Chem B 103:487
7. You H (2003) Abstracts of Papers, 225th ACS National Meeting, New Orleans, LA, 23-27 March 2003, COLL–488
8. Wang JX, Robinson IK, Ocko BM, Adzic RR (2005) J Phys Chem B 109:24
9. Santos E, Leiva EPM, Vielstich W (1991) Electrochim Acta 36:555
10. Love B, Lipkowski J (1988) ACS Symp Ser 378:484
11. Palaikis L, Zurawski D, Hourani M, Wieckowski A (1988) Surf Sci 199:183
12. Markovic NM, Schmidt TJ, Grgur BN, Gasteiger HA, Behm RJ, Ross PN (1999) J Phys Chem B 103:8568
13. Herrero E, Feliu JM, Blais S, Radovic-Hrapovic Z, Jerkiewicz G (2000) Langmuir 16:4779
14. Bergelin M, Herrero E, Feliu JM, Wasberg M (1999) J Electroanal Chem 467:74
15. Lebedeva NP, Koper MTM, Feliu JM, van Santen RA (2002) J Electroanal Chem 524:242
16. Lebedeva NP, Koper MTM, Feliu JM, van Santen RA (2002) J Phys Chem B 106:12938
17. Pozniak B, Mo Y, Scherson DA (2002) Faraday Discuss 121:313
18. Herrero, E Álvarez B, Feliu JM, Blais S, Radovic-Hrapovic Z, Jerkiewicz G (2004) J Electroanal Chem 567:139
19. Petukhov AV, Akemann W, Friedrich KA, Stimming U (1998) Surf Sci 402:182
20. Lebedeva NP, Rodes A, Feliu JM, Koper MTM, van Santen RA (2002) J Phys Chem B 106:9863
21. Koper MTM, Schmidt TJ, Markovic NM, Ross PN (2001) J Phys Chem B 105:8381
22. Angelucci CA, Nart FC, Herrero E, Feliu JM (2007) Electrochem Commun 9:1113
23. Strasser P, Eiswirth M, Ertl G (1997) J Chem Phys 107:991
24. Malkhandi S, Bonnefont A, Krischer K (2005) Electrochem Commun 7:710
25. Rodes A, Gómez R, Feliu JM, Weaver MJ (2000) Langmuir 16:811
26. Clavilier J, Armand D, Sun SG, Petit M (1986) J Electroanal Chem 205:267
27. Rodes A, El Achi K, Zamakhchari MA, Clavilier J (1990) J Electroanal Chem 284:245
28. Herrero E, Orts JM, Aldaz A, Feliu JM (1999) Surf Sci 444:259
29. García-Aráez N, Climent V, Herrero E, Feliu JM (2004) Surf Sci 560:269
30. Maciá MD, Campiña JM, Herrero E, Feliu JM (2004) J Electroanal Chem 564:141
31. Gómez R, Climent V, Feliu JM, Weaver MJ (2000) J Phys Chem B 104:597
32. Funtikov AM, Linke U, Stimming U, Vogel R (1995) Surf Sci 324:L343
33. Climent V, Gomez R, Feliu JM (1999) Electrochim Acta 45:629
34. Maciá MD, Herrero E, Feliu JM, Aldaz A (2001) J Electroanal Chem 500:498